nature photonics

LETTERS

PUBLISHED ONLINE: 25 JANUARY 2016 | DOI: 10.1038/NPHOTON.2015.276

Self-homodyne measurement of a dynamic Mollow triplet in the solid state

Kevin A. Fischer*†, Kai Müller†, Armand Rundquist, Tomas Sarmiento, Alexander Y. Piggott, Yousif Kelaita, Constantin Dory, Konstantinos G. Lagoudakis and Jelena Vučković*

The study of the light–matter interaction at the quantum scale has been enabled by the cavity quantum electrodynamics (CQED) architecture[1], in which a quantum two-level system strongly couples to a single cavity mode. Originally implemented with atoms in optical cavities[2,3], CQED effects are now also observed with artificial atoms in solid-state environments[4–6]. Such realizations of these systems exhibit fast dynamics, making them attractive candidates for devices including modulators and sources in high-throughput communications. However, these systems possess large photon out-coupling rates that obscure any quantum behaviour at large excitation powers. Here, we have used a self-homodyning[7] interferometric technique that fully employs the complex mode structure of our nanofabricated cavity[8–10] to observe a quantum phenomenon known as the dynamic Mollow triplet[11]. We expect this interference to facilitate the development of arbitrary on-chip quantum state generators, thereby strongly influencing quantum lithography, metrology and imaging.

The crowning achievement of quantum optics has been to develop a complete theory for the phenomenon of resonant light scattering from a quantized matter system. Beyond providing closure to debates over the nature of light, this theory has enabled observations of uniquely quantum spectacles such as photon anti-bunching[4,12], indistinguishable quantum interference[5,13] and the Mollow triplet[14,15]. The addition of nanoscale resonators to the quantum scattering problem has provided a new frontier in our quest to mould the flow of light[4–6]. Here, our reported innovation centres on the investigation of resonant light scattering from a quantum nonlinearity (quantum dot, QD) strongly coupled to a photonic-crystal cavity. This strong coupling allows for quantum-coherent energy exchange between the resonator's quantized light field and the QD's excitonic field, leading to the formation of light–matter entangled states known as polaritons[16–18]. Evidence for the system's strong coupling is provided from the clean avoided-crossing spectra in Fig. 1a. The relative positions of the emission peaks are determined by the transient energies of the Jaynes–Cummings (JC) ladder[19] (Fig. 1b). As the two polaritonic peaks transition through the avoided crossing (at the QD–cavity detuning of $\Delta_{\sigma a} = 0$), they change character from cavity/QD-like to QD/cavity-like. We now detail our unorthodox application of the full resonance structure in photonic crystals[8–10] to generate a self-homodyne interference[7] that emphasizes the hallmark quantum character of the scattered light.

In explaining landmark experiments from solid-state CQED with photonic crystals[6,16–18], only the fundamental cavity mode was considered to play a role. Recently, however, classical scattering studies of cross-polarized reflectivity through an L3 photonic-crystal cavity have suggested that the continuum modes above the light line may play an important role[8–10]. This additional scattering has been shown to interfere with the photonic crystal's fundamental cavity mode, resulting in a class of lineshape known as the Fano resonance[20]. To observe the typical background-free JC lineshape for a detuned strongly coupled system, we slightly defocused the sample to reject the continuum mode scattering[8,9] from the L3 photonic crystal. Figure 1c presents the results of a broadband cross-polarized reflectivity (identical to transmission) experiment[18]. This measurement is a cut from Fig. 1a at $\Delta_{\sigma a} = -85$ pm and shows a

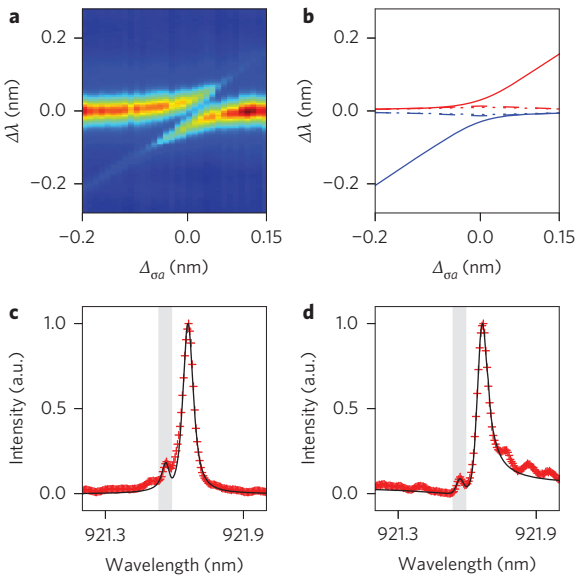

Figure 1 | Characterization of the strongly coupled system. a, Cross-polarized reflectivity (mimicking transmission) spectrum of the coupled QD–cavity system obtained when tuning the QD resonance through the cavity mode. By fitting profiles from these spectra, we extract the cavity energy decay rate $\kappa = 2\pi \times 15$ GHz and the coherent coupling rate $g = 2\pi \times 11$ GHz. **b**, Transient energies for climbing the JC ladder, rung by rung, for the first, second and third rung, shown as solid, dashed and dotted lines, respectively. Transitions from upper and lower polaritons are colour-coded in red and blue, respectively. **c**,**d**, Spectra of the coupled QD–cavity system taken at a QD–cavity detuning of $\Delta_{\sigma a} = -85$ pm and an excitation power of ~15 nW nm^{-1}, showing QD-like polaritonic emission (highlighted in grey) on top of a Lorentzian resonance (**c**) and a Fano resonance (**d**). In both cases, spectra are taken by performing broadband cross-polarized reflectivity measurements on the system, but under different interference conditions (with altered focus). Red hashes indicate experimental data and black curves indicate quantum-optical fits.

E.L. Ginzton Laboratory, Stanford University, Stanford, California 94305, USA. †These authors contributed equally to this work.
*e-mail: kevinf@stanford.edu; jela@stanford.edu

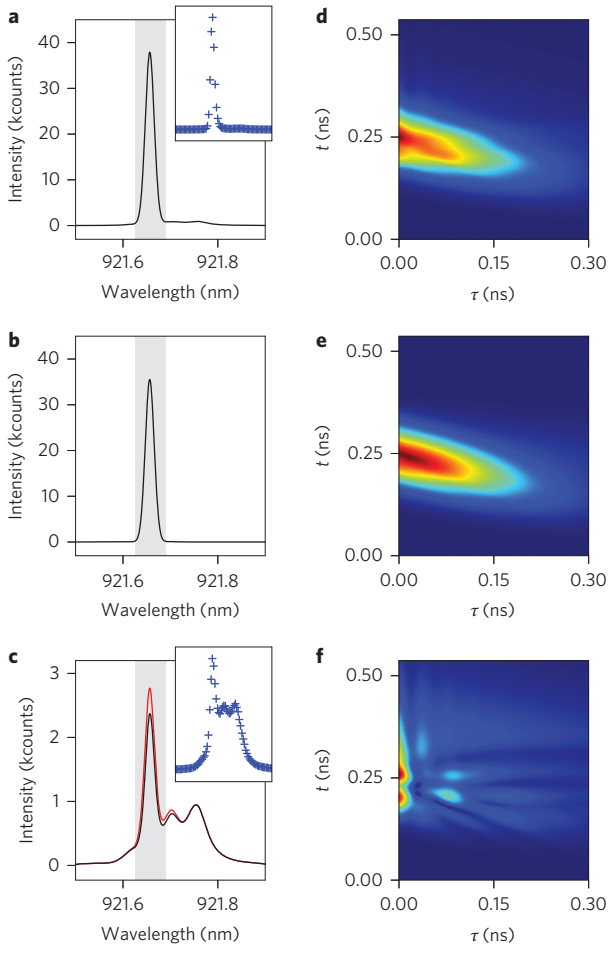

Figure 2 | Evidence for Fano-induced self-homodyne interference from the detuned strongly coupled system. First-order correlations and their spectra under resonant excitation of the QD-like polariton (at the centre of the grey shading) with an 80 MHz repetition rate pulsed laser with FWHM $\tau_p = 100$ ps. **a**, Simulated spectrum of total emission from the JC system. Inset: Experimental data taken at 500 nW incident power and the interference condition yielding the Lorentzian-like resonance in Fig. 1c (Supplementary Fig. 1). Note that the inset shares axes with the main panel. **b**, Simulated spectrum of coherently scattered light from the same JC system under identical excitation. **c**, Simulated spectrum of incoherently scattered light (black), and simulated spectrum interfering the JC emission with the continuum-mode emission (red), revealing the incoherently scattered light. Inset: Experimental data taken at 500 nW incident power and the interference condition yielding the Fano-like resonance in Fig. 1d (Supplementary Fig. 1). Note that the inset shares axes with the main panel. **d**–**f**, Simulated two-time correlation functions $\langle A^\dagger(t+\tau)A(t)\rangle$ corresponding to the spectra in **a**–**c**, respectively. Plots **d** and **e** show few differences, but self-homodyne interference reveals the rich correlations in **f** due to quantum fluctuations.

small hump of QD-like polaritonic emission on top of a Lorentzian cavity-like resonance. An excellent fit (black line) is obtained with a quantum-optical JC transmission model[19,21] (see Methods).

Next, we returned the sample focus to again destructively interfere the cavity and continuum channels. We now show experimentally that the inclusion of this continuum-mode scattering can interferometrically reject scattered light from the cavity-like polariton in favour of emission from the QD-like polariton. The resulting lineshape (Fig. 1d) shows QD-like polaritonic emission on top of a Fano resonance. Importantly, by comparing this result to Fig. 1c, we see that emission from the cavity-like polariton at the QD-like polaritonic emission wavelength is significantly suppressed (Supplementary Figs 2 and 3). Although previous experiments have used homodyne interference to create Fano-like lineshapes with QD–photonic crystal cavity systems[22], the interference was not capable of reducing light scattered from the cavity-like polariton in favour of emission from the QD-like polariton. In contrast, our unconventional technique enables the continuum modes to interfere with nearly the exact opposite phase from that of the cavity mode, leading to an apt description: Fano-induced self-homodyne interference. By analogy to a traditional homodyne measurement, this interference allows for the extraction of hidden signals.

Next, we explore the implications of this suppression at high excitation powers and show that only light from the cavity-like polariton is interferometrically cancelled at the QD-like polariton's emission frequency. To this end, we performed simulations and experiments in which we resonantly excited the system at the QD-like polariton's emission frequency with a laser pulse. In a formal quantum-mechanical description of scattering[23], the spectrum of the free-field mode operator $A(t)$ as measured by an ideal infinite-bandwidth detector is given by

$$S(\omega) = \iint_{R^2} \mathrm{d}t\mathrm{d}\tau \mathrm{e}^{-\mathrm{i}\omega\tau}\langle A^\dagger(t+\tau)A(t)\rangle \qquad (1)$$

integrating over all possible two-time correlations $\langle A^\dagger(t+\tau)A(t)\rangle$.

When computing expectations for combinations of $A(t)$ (Supplementary Section 'Temporal and spectral filtering'), input–output theory[7] can relate the internal cavity mode operator $a(t)$ to the external field operator by the radiative cavity field coupling rate $\kappa/2$. Hence, for a JC system in the solid state where the QD radiative lifetime plays an insignificant role compared to κ (ref. 24), spectral decomposition of the cavity mode operator yields the spectrum of the detected light. Therefore, we can compute an unnormalized version of this spectrum with $A(t) \to a(t)$ in equation (1). In the inset of Fig. 2a, we present experimental data (without Fano filtering) in agreement with this model: only a single peak at the QD-like polaritonic wavelength is observed. Next, we compute the coherent spectrum[23] of the light scattered from the JC system (Fig. 2b); the coherent spectrum is computed with $\langle A^\dagger(t+\tau)A(t)\rangle \to \langle a^\dagger(t+\tau)\rangle\langle a(t)\rangle$ in equation (1). Aside from the similarity of Fig. 2a and b, the two-time correlations in Fig. 2d,e from which the spectra in Fig. 2a,b are (respectively) derived, exhibit nearly identical profiles. These strong similarities suggest that the scattered light from our JC system at high powers is mostly coherent and thus predominantly classical in nature.

On the other hand, the incoherently scattered light reveals the effect of the embedded quantum nonlinearity. The JC incoherent spectrum, the spectrum of cavity-mode operator fluctuations[23] (black line in Fig. 2c), is simulated with

$$\langle A^\dagger(t+\tau)A(t)\rangle \to \langle a^\dagger(t+\tau)a(t)\rangle - \langle a^\dagger(t+\tau)\rangle\langle a(t)\rangle \qquad (2)$$

in equation (1) and clearly shows massive nonlinear conversion at a single-photon level as well as rich quantum character in the two-time correlations (Fig. 2f). Strikingly, by careful manipulation of the continuum-mode channel (aforementioned) to enable self-homodyne suppression of the coherently scattered light, we obtain an experimental spectrum (inset of Fig. 2c) remarkably close to the simulated incoherent spectrum. We note that this measurement is extremely phase-stable due to the self-homodyne interference. Note that the left- and rightmost peaks occur at the QD-like and cavity-like polaritons (Fig. 1d), respectively (the middle peak will be discussed later).

By comparing the spectra in Fig. 2a and c, we find that we are experimentally capable of rejecting >95% of the coherently scattered light at this detuning. To model this effect, we replace the free-field

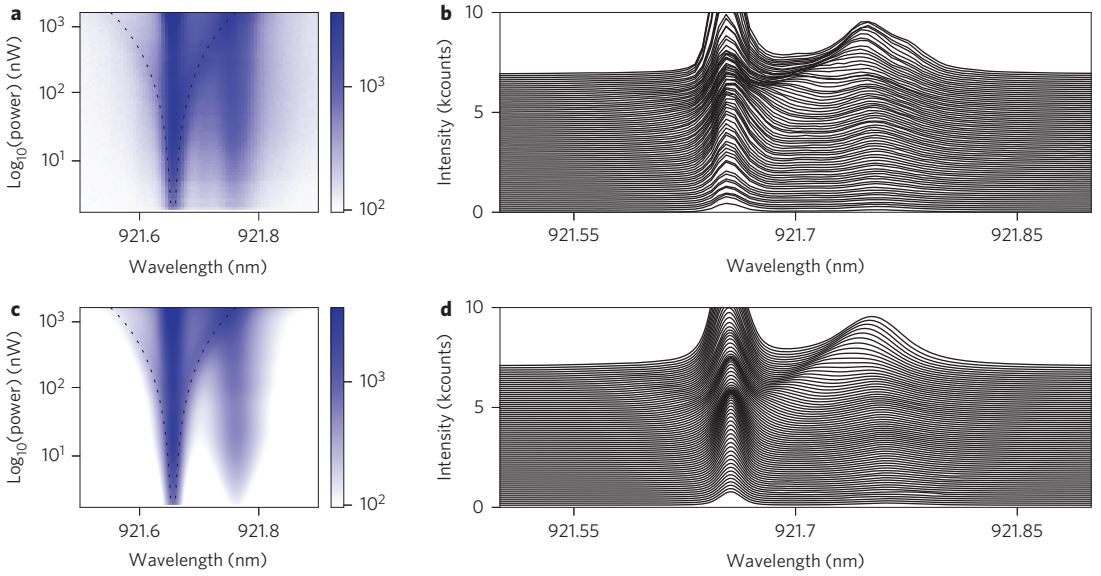

Figure 3 | Emergence of dynamic Mollow-like triplets from the detuned strongly coupled system under pulsed resonant excitation of the QD-like polariton. a,**b**, Experimental power-series spectra of emission from our system, with self-homodyne interference, as a function of the average power from the $\tau_p = 100$ ps FWHM pulsed excitation laser. The data are plotted on a log plot (**a**) and as stacked spectra (**b**): the log plot easily shows the power dependence of the sideband frequencies, while the stacked spectra reveal strong suppression due to interference. Note that these spectra are taken at the same QD–cavity detuning as the spectra in Fig. 2. Here, two Mollow-like sidebands clearly emerge with increasing excitation power. The presence of the cavity, combined with acoustic phonon scattering, leads to a dramatic asymmetry in the emission from the two sidebands. **c**,**d**, Simulated power-series spectra, plotted on the same scale and in the same manner as in **a** and **b**, showing excellent agreement in both qualitative shape and quantitative values with the experimental data in **a** and **b**. Dashed lines show a fit to the power dependence of the triplet frequency splittings (Supplementary Section 'Power dependence of the dynamic Mollow triplet'). Self-homodyne interference clearly reveals and enables the measurement of these unique incoherent scattering spectra from a highly dissipative strongly coupled system.

operator with a superposition of the cavity mode operator and the scattered coherent state $\alpha(t)$, that is, $A(t) \rightarrow a(t) + \alpha(t)$ in equation (1) (red line in Fig. 2c). Physically, $\alpha(t)$ is a slightly phase- and amplitude-shifted version of the incident laser pulse (originating from the continuum-mode scattering). For a proper choice of $\alpha(t)$, the simulated experimental spectrum is nearly identical to the JC incoherent spectrum. From the excellent agreement between simulation and experiment, we conclude that our Fano-induced self-homodyne measurement leads almost exclusively to the incoherent portion of the strongly coupled system's spectrum.

Armed with the self-homodyne technique, we sought an application to demonstrate its ability to reveal interesting quantum optics, and we chose to investigate the theoretically predicted dynamic Mollow triplets that arise under the pulsed excitation of a solid-state system[11]. We emphasize that this effect is quite different from the conventional Mollow triplets (already studied in the solid state[15]) that are observed under strong resonant continuous-wave driving of a two-level system. Specifically, the dynamic Mollow triplets that emerge under pulsed resonant driving of a two-level system have not yet been observed in the solid state, as they require excitation laser pulse durations longer than the state lifetime with very high powers[11]. Here, we chose the QD-like polariton of our CQED system as the two-level system to be driven, because its strong coupling to the cavity provides a solution to these excitation challenges: the cavity coupling decreases the QD state lifetime, and the high-quality-factor cavity increases polariton coupling to the probe field. Hence, we can observe the formation of dynamic Mollow triplets with driving laser pulses of $\tau_p = 100$ ps, only approximately two times longer than the QD-like polariton lifetime. Uniquely in the strongly coupled system, as Fig. 1b suggests, some detuning is required to generate enough nonlinearity in the JC ladder to drive relatively clear two-photon transitions. These cavity enhancements come at the cost of increased coherent scattering, which obscures the Mollow triplets, as seen in Fig. 2, so we are required to use the self-homodyne technique to reveal this quantum effect.

The striking experimental observation of dynamic Mollow-triplet sidebands is shown in Fig. 3a,b. The sideband frequencies follow the square root of the probe power, as derived for the detuned CQED system (Supplementary Section 'Power dependence of the dynamic Mollow triplet'). Experimentally, we found the triplets most clear at $\Delta_{\sigma a} = -85$ pm. Interestingly, the Mollow-like sidebands are extremely unbalanced: emission at the cavity-like polariton frequency occurs for all powers due to interaction with the higher JC manifolds, which is emphasized by exciton–phonon interaction[25]. These features are shown to be in excellent agreement with a quantum optical simulation of dynamic Mollow triplets from the CQED system with self-homodyne Fano interference (Fig. 3c,d). Simulations suggest that the maximum cavity occupancy during CQED triplet production is only 1.5–2 photons with a variance of <0.2, strongly distinguishing the CQED triplets from those arising under the strong-pump limit of a CQED system that leads to the traditional Mollow triplet[26]. Additionally, the strong-coupling-induced asymmetry of the CQED dynamic triplet masks the presence of the additional side peaks theoretically predicted from a two-level system[11] (Supplementary Fig. 4).

Thus, we have demonstrated a Fano-induced self-homodyne measurement technique and used it to observe a unique CQED phenomenon in the solid state—the dynamic Mollow triplet. Hence, we have been able to probe a highly dissipative JC system in a high-pulse-energy regime for the first time, and expect this technique to allow for a more thorough exploration of the rich JC dynamics in solid-state systems. The observation of this phenomenon even has practical relevance to the emerging field of Mollow spectroscopy, where the dynamic Mollow triplets may serve as ultrasensitive probes for the nonlinearity of new quantum emitters[27]. Furthermore, we expect the ability to use the self-homodyne technique to stably measure quantum fluctuations to find application

in the generation of other arbitrary quantum states of light. In particular, we have already shown that our interferometric measurement methodology enables nearly perfect single-photon generation in solid-state photon blockade[24], and believe that it will also enable the first generation of indistinguishable photons from an optical solid-state CQED system. Furthermore, the ability to mitigate unwanted coherent scattering from highly dissipative JC systems should facilitate the direct observation of the JC higher rungs, and thus it may allow for low-detuning photon bundling[28] of arbitrary photon number states, with applications in quantum lithography, metrology and microscopy. In fact, self-homodyne interference may prove extremely valuable in designing on-chip sources of quantum light, where almost any waveguide-coupled cavity can easily exploit Fano interference[29]. Therefore, in looking toward future applications, our approach may play a pivotal role in generating quantum light while overcoming the inherently strong dissipation of solid-state systems.

Methods

Methods and any associated references are available in the online version of the paper.

Received 3 April 2015; accepted 10 December 2015; published online 25 January 2016

References

1. Haroche, S. & Kleppner, D. Cavity quantum electrodynamics. *Phys. Today* **42,** 24 (January, 1989).
2. Nußmann, S. *et al.* Vacuum-stimulated cooling of single atoms in three dimensions. *Nature Phys.* **1,** 122–125 (2005).
3. Birnbaum, K. M. *et al.* Photon blockade in an optical cavity with one trapped atom. *Nature* **436,** 87–90 (2005).
4. Michler, P. *et al.* A quantum dot single-photon turnstile device. *Science* **290,** 2282–2285 (2000).
5. Santori, C., Fattal, D., Vucković, J., Solomon, G. S. & Yamamoto, Y. Indistinguishable photons from a single-photon device. *Nature* **419,** 594–597 (2002).
6. Faraon, A. *et al.* Coherent generation of non-classical light on a chip via photon-induced tunnelling and blockade. *Nature Phys.* **4,** 859–863 (2008).
7. Carmichael, H. J. *Statistical Methods in Quantum Optics* (Springer, 2008).
8. Vasco, J. P., Vinck-Posada, H., Valentim, P. T. & Guimãraes, P. S. S. Modeling of Fano resonances in the reflectivity of photonic crystal cavities with finite spot size excitation. *Opt. Express* **21,** 31336–31346 (2013).
9. Galli, M. *et al.* Light scattering and Fano resonances in high-*Q* photonic crystal nanocavities. *Appl. Phys. Lett.* **94,** 071101 (2009).
10. Valentim, P. T. *et al.* Asymmetry tuning of Fano resonances in GaAs photonic crystal cavities. *Appl. Phys. Lett.* **102,** 111112 (2013).
11. Moelbjerg, A., Kaer, P., Lorke, M. & Mørk, J. Resonance fluorescence from semiconductor quantum dots: beyond the Mollow triplet. *Phys. Rev. Lett.* **108,** 017401 (2012).
12. Kimble, H. J., Dagenais, M. & Mandel, L. Photon antibunching in resonance fluorescence. *Phys. Rev. Lett.* **39,** 691–695 (1977).
13. Hong, C. K., Ou, Z. Y. & Mandel, L. Measurement of subpicosecond time intervals between two photons by interference. *Phys. Rev. Lett.* **59,** 2044–2046 (1987).
14. Mollow, B. R. Power spectrum of light scattered by two-level systems. *Phys. Rev.* **188,** 1969–1975 (1969).
15. Flagg, E. B. *et al.* Resonantly driven coherent oscillations in a solid-state quantum emitter. *Nature Phys.* **5,** 203–207 (2009).
16. Yoshie, T. *et al.* Vacuum Rabi splitting with a single quantum dot in a photonic crystal nanocavity. *Nature* **432,** 200–203 (2004).
17. Reithmaier, J. P. *et al.* Strong coupling in a single quantum dot–semiconductor microcavity system. *Nature* **432,** 197–200 (2004).
18. Englund, D. *et al.* Controlling cavity reflectivity with a single quantum dot. *Nature* **450,** 857–861 (2007).
19. Laussy, F. P., del Valle, E., Schrapp, M., Laucht, A. & Finley, J. J. Climbing the Jaynes–Cummings ladder by photon counting. *J. Nanophoton.* **6,** 061803 (2012).
20. Fano, U. Effects of configuration interaction on intensities and phase shifts. *Phys. Rev.* **124,** 1866–1878 (1961).
21. Alsing, P., Guo, D. & Carmichael, H. J. Dynamic stark effect for the Jaynes-Cummings system. *Phys. Rev. A* **45,** 5135–5143 (1992).
22. Fushman, I. *et al.* Controlled phase shifts with a single quantum dot. *Science* **320,** 769–772 (2008).
23. Wilkens, M. & Rzaewski, K. Resonance fluorescence of an arbitrarily driven two-level atom. *Phys. Rev. A* **40,** 3164–3178 (1989).
24. Müller, K. *et al.* Ultrafast polariton–phonon dynamics of strongly coupled quantum dot–nanocavity systems. *Phys. Rev. X* **5,** 031006 (2015).
25. Roy, C. & Hughes, S. Polaron master equation theory of the quantum-dot Mollow triplet in a semiconductor cavity–QED system. *Phys. Rev. B* **85,** 115309 (2012).
26. Cohen-Tannoudji, C. *Atom–Photon Interactions* (Wiley, 2004).
27. López Carreño, J. C., Sánchez Muñoz, C., Sanvitto, D., del Valle, E. & Laussy, F. P. Exciting polaritons with quantum light. *Phys. Rev. Lett.* **115,** 196402 (2015).
28. Sánchez Muñoz, C. *et al.* Emitters of *N*-photon bundles. *Nature Photon.* **8,** 550–555 (2014).
29. Yu, Y. *et al.* Fano resonance control in a photonic crystal structure and its application to ultrafast switching. *Appl. Phys. Lett.* **105,** 061117 (2014).

Acknowledgements

The authors acknowledge financial support from the Air Force Office of Scientific Research, the MURI Center for Multifunctional Light–Matter Interfaces based on Atoms and Solids, and support from the Army Research Office (grant no. W911NF1310309). K.A.F. acknowledges support from the Lu Stanford Graduate Fellowship and the National Defense Science and Engineering Graduate Fellowship. K.M. acknowledges support from the Alexander von Humboldt Foundation. A.Y.P. acknowledges support from the Bechtolsheim Stanford Graduate Fellowship. Y.A.K. acknowledges support from the Stanford Graduate Fellowship and the National Defense Science and Engineering Graduate Fellowship. K.G.L. acknowledges support from the Swiss National Science Foundation.

Author contributions

K.A.F. and K.M. conceived and performed the experiments. K.A.F. performed the theoretical work and modelling. A.R. fabricated the device. T.S. performed MBE growth of the QD structure. A.P., Y.A.K., C.D. and K.G.L. provided expertise. J.V. supervised the project. All authors participated in the discussion and understanding of the results.

Additional information

Supplementary information is available in the online version of the paper. Reprints and permissions information is available online at www.nature.com/reprints. Correspondence and requests for materials should be addressed to K.A.F. and J.V.

Competing financial interests

The authors declare no competing financial interests.

Methods

The MBE-grown structure consisted of an approximately 900-nm-thick $Al_{0.8}Ga_{0.2}As$ sacrificial layer followed by a 145-nm-thick GaAs layer that contained a single layer of InAs QDs. Our growth conditions resulted in a typical QD density of 60–80 μm^{-2}. Using 100 keV electron-beam lithography with ZEP resist, followed by reactive ion etching and HF removal of the sacrificial layer, we defined the photonic-crystal cavity. The photonic-crystal lattice constant was $a = 246$ nm and the hole radius was $r \approx 60$ nm. The cavity fabricated was a linear three-hole defect (L3) cavity. To improve the cavity quality factor, holes adjacent to the cavity were shifted.

All optical measurements were performed with a liquid-helium flow cryostat at a temperature of ~30 K. A 1.0-m-long pulse shaper was used to generate experimental excitation pulses from a 3 ps Tsunami mode-locked laser. For excitation and detection, a microscope objective with a numerical aperture of NA = 0.75 was used. Cross-polarized measurements were performed using a polarizing beamsplitter. To further enhance the extinction ratio, additional thin-film linear polarizers were placed in the excitation/detection pathways, and a single-mode fibre was used to spatially filter the detection signal. Two wave plates were placed between the beamsplitter and microscope objective: a half-wave plate to rotate the polarization relative to the cavity and a quarter-wave plate to correct for birefringence of the optics.

Quantum-optical simulations were performed with the Quantum Optics Toolbox in Python (QuTiP)[30], where the standard[21] JC model was used as a starting point. For the JC transmission experiments, the cavity occupancy was monitored as the excitation frequency was swept. The scattered coherent state was included through a time-independent operator replacement similar to the one discussed in the main text. The effects of phonons were incorporated through the addition of incoherent decay channels and were subsequently used as fitting parameters. Effective phonon-transfer rates for the $a^{\dagger}\sigma$ and the $a\sigma^{\dagger}$ processes were $2\pi \times 0.9$ GHz and $2\pi \times 0.65$ GHz, respectively. These rates are consistent with previous experimental results and a more rigorous analysis[24].

References

30. Johansson, J., Nation, P. & Nori, F. Qutip: an open-source python framework for the dynamics of open quantum systems. *Comput. Phys. Commun.* **183,** 1760–1772 (2012).